

# Improvement of Bondability by Depressing the Inhomogeneous Distribution of Nanoparticles in a Sintering Bonding Process with Silver Nanoparticles

JIANFENG YAN,<sup>1,3</sup> GUISHENG ZOU,<sup>1</sup> AIPING WU,<sup>1</sup> JIALIE REN,<sup>1</sup>  
ANMING HU,<sup>2</sup> and Y. NORMAN ZHOU<sup>1,2</sup>

1.—Department of Mechanical Engineering & Key Laboratory for Advanced Manufacturing by Materials Processing Technology, Ministry of Education of P. R. China, Tsinghua University, Beijing 100084, China. 2.—Department of Mechanical and Mechatronics Engineering, Centre of Advanced Materials for Joining, University of Waterloo, 200 University Avenue West, Waterloo, ON N2L 3G1, Canada. 3.—e-mail: yanjf09@mails.tsinghua.edu.cn

Low-temperature bonding by sintering of Ag nanoparticles (NPs) is a promising lead-free bonding technique used in the electronic packaging industry. In this work, we prepare Ag nanoparticle (NP) paste using both an aqueous method and a polyol method. Sintering bonding trials were then conducted using different forms of Ag NPs. The results showed that use of the aqueous-based Ag NP paste led to inhomogeneous distribution of NPs, known as the “coffee-ring effect.” This led to low strength of fabricated joints. We investigated the influence of the coffee-ring effect and ways to depress it by changing the bonding material composition. Our results show that, when using polyol-based Ag NP paste as the bonding material, the coffee-ring effect was successfully depressed due to increased Marangoni flow. The corresponding shear strength of joints was increased significantly to 50 MPa at bonding temperature of 250°C.

**Key words:** Ag nanoparticles, coffee-ring effect, bondability, electronic packaging

## INTRODUCTION

Sn–Pb-based alloy solders have been used extensively for many years in microelectronic assemblies. However, lead and its compounds are toxic and are known to have a detrimental effect on the environment and human health. Emerging regulations have targeted elimination of Pb usage from electronic assemblies in many countries.<sup>1,2</sup> This background has stimulated substantial research and development efforts to discover substitute lead-free solder alloys.<sup>3</sup> Although many Pb-free solder alloy compositions (Sn–Ag, Sn–Cu, etc.) have been proposed, thus far, none meets all requirements.<sup>2,3</sup> In particular, there are no suitable lead-free high-temperature solders. High-temperature solders containing 90 wt.% to 95 wt.% Pb are still widely

used in various applications.<sup>4</sup> Therefore, there is a strong drive to find Pb-free alternatives for high-temperature applications.

Recently, there has been an increasing focus on developing solid-state bonding interconnection processes based on sintering, as an alternative to solder melting, to provide a novel lead-free bonding technology. Nanojoining, especially nanoscopic diffusion bonding using metallic nanoparticles (Ag, Cu, etc.), has significant advantages over conventional soldering or adhesive bonding.<sup>5–8</sup> Ag has high electrical and thermal conductivity and exhibits good fatigue performance. These good properties as well as its high melting point (960°C) make Ag a suitable material for high-temperature packaging applications.

Due to the size effect, silver nanoparticles can be sintered at low temperature and have potential as a Pb-free, high-performance interconnect material for high-temperature electronic applications.<sup>6,9</sup> These lead-free bonding materials will not pollute the

(Received August 16, 2011; accepted January 27, 2012;  
published online March 7, 2012)

environment or harm human health. Moreover, this low-temperature interconnection technology has potential applications for flexible electronics.<sup>7,8,10</sup> However, there are still some problems to be solved for its practical application. Formation of robust joints at lower bonding temperature and bonding pressure is still needed. In particular, deposition of uniform layers of Ag nanoparticles is critical for formation of robust joints using this bonding process. Recent work from our and other groups has shown that sintering bonding technology using metal nanoparticles as the bonding material is influenced by the coffee-ring effect.<sup>11,12</sup> In this sintering bonding process using Ag nanoparticle paste, the inhomogeneous distribution of aqueous-based Ag NP paste related to this coffee-ring effect will affect the bonding quality of the joint. This coffee-ring effect is a phenomenon of colloid solutions due to different evaporation rates of solvents, which may push the suspension of particles to the wetting edge. When such a coffee ring appears, joint strength may be dramatically reduced due to the reduced connection area. However, there are few reports about the influence of the coffee-ring effect on sintering bonding technology using Ag nanoparticle paste. Thus, it is necessary to investigate the influence of and how to control the coffee-ring effect in order to increase joint strength.

In this study, both aqueous-based Ag nanoparticle paste and polyol-based Ag nanoparticle paste were used for this sintering bonding application. Our results show that, when using polyol-based Ag NP paste as the bonding material, the coffee-ring effect is successfully depressed due to increased Marangoni flow. The corresponding shear strength of joints was significantly increased.

## EXPERIMENTAL PROCEDURES

### Preparation of Ag Nanoparticles

Polyvinylpyrrolidone (PVP.K30), silver nitrate ( $\text{AgNO}_3$ ), deionized (DI) water, ethylene glycol (EG), acetone, and ethanol were all of analytical grade and used without further purification.

The Ag nanoparticles (in the form of paste) used in this study were prepared by aqueous and polyol methods as follows:

- (i) The aqueous-based Ag nanoparticles Ag nanoparticles were synthesized through a chemical reduction reaction of  $\text{AgNO}_3$  using sodium citrate dehydrate as reducing agent. Details of the synthesis procedure have been presented in a previous study.<sup>12</sup> A solution of  $\text{AgNO}_3$  (1 mM) in 250 mL ultrapure water was heated to 80°C. A volume of 10 mL aqueous solution of  $\text{Na}_3\text{C}_6\text{H}_5\text{O}_7 \cdot 2\text{H}_2\text{O}$  (0.34 mM) was then added to the  $\text{AgNO}_3$  solution. Heating was continued to 90°C for 30 min after adding the citrate solution. The color of the solution changed from the colorless water to yellow after 15 min of heating,

and to gray after 25 min. The resulting sol is simply silver NPs coated with organic shell, dispersed in water at concentration of 1 mM. The silver NP paste was fabricated by increasing the concentration of the silver nanoparticle solution from 1 mM to 0.1 M by centrifugation. Centrifugation was conducted at 7000 revolutions per minute (rpm) for 20 min in 15-mL centrifuge tubes (length 118.54 mm, outer diameter 15.62 mm). The water was extracted from the centrifuge tubes using a pipette, leaving aqueous-based Ag nanoparticle paste at the bottom. Ag nanoparticle powder was prepared by drying the aqueous-based Ag nanoparticle paste. The aqueous-based Ag nanoparticles were baked at 60°C in a glass beaker. The Ag nanoparticle powder accumulated at the bottom of the glass beaker and was collected using a clean spatula.

- (ii) The polyol-based Ag nanoparticles were synthesized by the polyol process.<sup>13</sup> The typical synthesis method is described as follows: First, 10 mL EG solution of silver nitrite (0.15 M) in a conical flask and 40 mL ethylene glycol solution of PVP (0.45 M) in a beaker were prepared. Second, these solutions were heated at constant heating rate of 20°C/min to the reaction temperature of 160°C. Then, the solution of PVP was injected into the silver nitrite solution at constant rate of 0.3 mL/s using a syringe pump. The color of the solution changed from colorless water to gray after 30 min, indicating precipitation of Ag NPs. When the reaction was complete, the solution was rapidly cooled by adding DI water to 200 mL. The silver NP paste (denoted as polyol-based Ag nanoparticle paste) was obtained by centrifugation using a similar method as above (i).

### Bonding Procedure

To evaluate the bondability of different Ag nanoparticles (in the form of paste) and Ag nanoparticle powder, Ni/Ag-plated Cu discs were bonded using different Ag nanoparticles under the same conditions. The Ni/Ag-plated copper discs were made by first plating a layer of nickel on the copper discs, then silver plating was applied over the nickel plating. Figure 1 shows a schematic of the bonding specimens. The Ni/Ag-plated copper discs were ultrasonic washed using acetone and ethanol solutions before

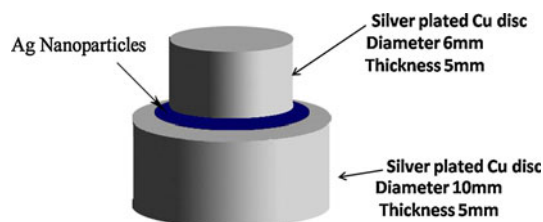


Fig. 1. Schematic of the bonding specimens.

use. A layer of Ag nanoparticles (in the form of paste or powder) was sandwiched between the two Ni/Ag-plated copper discs. Ag nanoparticle paste was placed on the copper substrates using a syringe with a needle. Afterwards, these prepared bonding specimens were heated to the bonding temperature of 250°C in air under bonding pressure of 5 MPa and held for 30 min.

### Characterization Techniques

The morphology of the Ag nanoparticles was examined by field-emission scanning electron microscopy (SEM). To study the deposition behaviors of the Ag nanoparticle paste synthesized by the aqueous or polyol method, Ag nanoparticle pastes were deposited on the Cu substrate using a syringe with a needle. The deposited Ag layers were dried at 60°C. The deposited Ag layers and cross-sectional images of the joints were examined by optical microscopy. The surface profiles of the deposited Ag layers were measured using a Talysurf 5P-120 topographer. The shear strengths of three joints for each condition were measured using the thermal-mechanical simulator Gleeble 1500D at displacement speed of 5 mm/min at room temperature. The shear strength was then taken as the maximum load divided by the lower surface area of the small Cu disc.

## RESULTS AND DISCUSSION

### Characteristics of Ag NPs

Figure 2a, b displays Ag nanoparticles synthesized by the aqueous and polyol methods. Figure 2c shows the Ag nanoparticle powder dried from the aqueous Ag nanoparticle solution. As shown in Fig. 2a, Ag nanoparticles synthesized by the aqueous method were spherical, having mean size of about 45 nm. The Ag nanoparticles synthesized by the polyol method had diameter of about 40 nm, as shown in Fig. 2b. As shown in Fig. 2c, the deposited powder was microscale pellets with flake shape. Under higher magnification (inset to Fig. 2c), these microscale silver flakes consisted of tightly packed silver nanoparticles.

### Deposition Behaviors of Ag Nanoparticle Paste

In terms of obtaining high-quality joints, uniform deposition of the Ag nanoparticles before joint assembly and bonding is critical. The deposition behaviors of Ag nanoparticle pastes synthesized by the two methods were compared. Aqueous Ag nanoparticles and polyol Ag nanoparticles with the same amount (0.09 mmol Ag NP paste) were placed on copper substrates with the needle syringe. Then, the two kinds of concentrated Ag nanoparticle pastes were evaporated simultaneously at the same conditions (60°C) in air. After drying, the deposited Ag nanoparticles resulted in a circular coated area with 3000  $\mu\text{m}$  to 5000  $\mu\text{m}$  diameter.

Figure 3 shows optical images and corresponding two-dimensional profiles of the Ag layers deposited on copper substrates. When using Ag nanoparticles synthesized by the aqueous method, the deposited Ag layer exhibited a typical narrow edge with a remarkable height surrounding a flat central area. As displayed in Fig. 3a, silver nanoparticles accumulated at the rim of the deposited area while the central region was almost empty. This uneven distribution of Ag nanoparticles is related to the coffee-ring effect.<sup>14</sup> When a droplet of Ag nanoparticle paste is placed on the substrate surface, the evaporation flux distribution along the droplet surface is not uniform. The evaporation rate is larger at the edge than that at the center,<sup>15</sup> thus more water evaporated from the edge region. However, during the evaporation process the radius of the droplet of Ag nanoparticle paste cannot shrink, as its contact line is pinned. During the evaporation of water from the Ag nanoparticle paste at the droplet edge, the water lost must be replaced by water drawn from the center of the droplet. This flow that brings fluid from the center to the edge of the droplet also carries many Ag nanoparticles, which results in the coffee-ring effect. Most of the suspended Ag nanoparticles are segregated at the edge, while a few silver nanoparticles settle in the central region of the ring. This leads to the characteristic coffee-ring shape of the deposited Ag layer, as displayed in Fig. 3a.

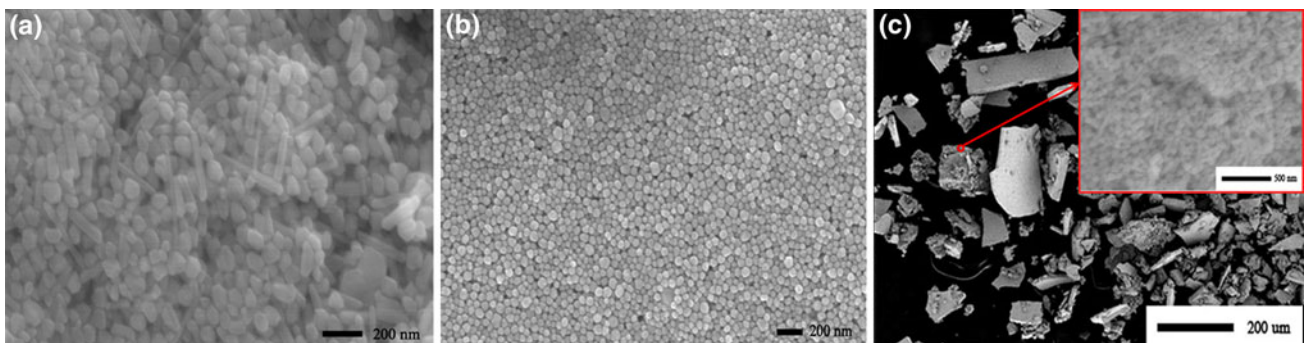


Fig. 2. SEM images of Ag NPs: (a) aqueous Ag nanoparticles, (b) polyol-based Ag nanoparticles, and (c) Ag nanoparticle powder.

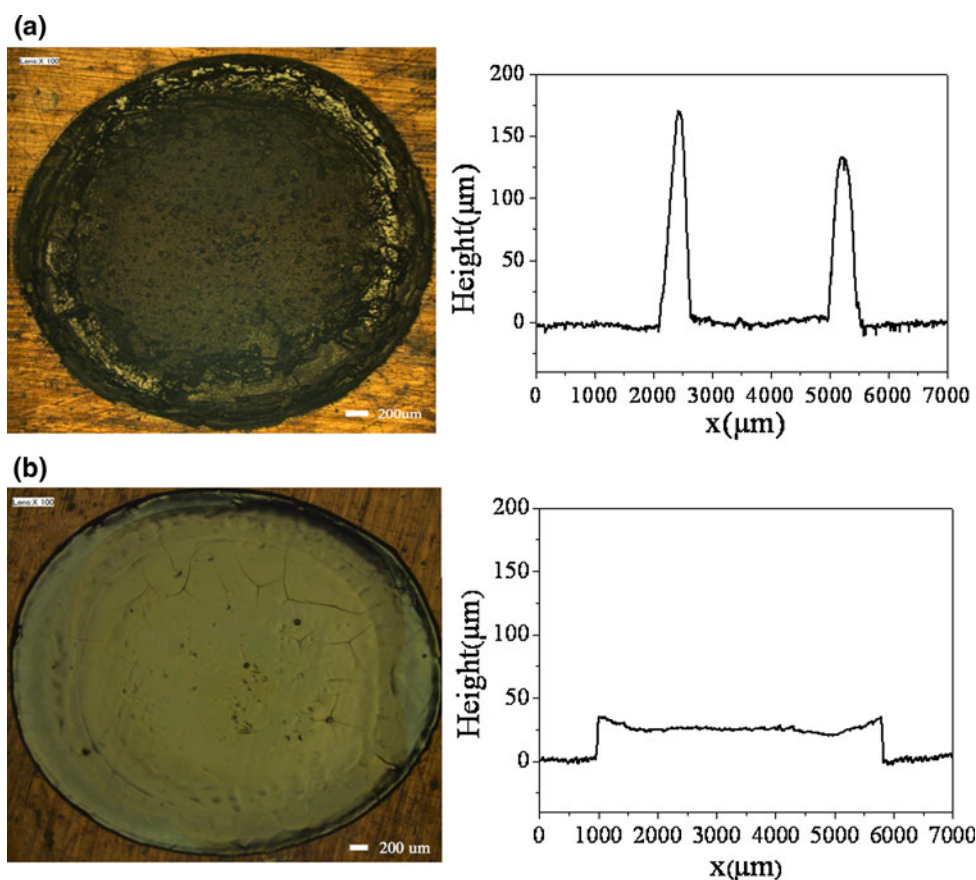


Fig. 3. Optical images and corresponding two-dimensional profiles of different deposited Ag layers: (a) aqueous Ag nanoparticle paste, and (b) polyol-based Ag nanoparticle paste.

On the other hand, this coffee-ring effect was successfully reduced during the drying of the polyol Ag nanoparticles. As shown in Fig. 3b, the deposited Ag layer showed relatively flat and uniform shape without obvious segregation. The elimination of the coffee-ring effect was due to the generation of Marangoni flow, which is induced by incorporating a solvent with low boiling point and high surface tension.<sup>16</sup> For the polyol Ag nanoparticle paste, the solvent is mixed water and ethylene glycol (EG). The water and EG have different volatilities and surface tensions (water: boiling temperature  $T_b = 100^\circ\text{C}$ , surface tension  $\gamma = 72.8 \text{ mN/m}$ ; EG:  $T_b = 197^\circ\text{C}$ , surface tension  $\gamma = 48.5 \text{ mN/m}$ ). The differences in volatilities and surface tensions between the water and EG may induce Marangoni flow.<sup>17</sup> For the polyol-based Ag nanoparticle paste, the initial enhanced evaporation of EG not only induces convective flow but also leads to the development of a concentration gradient of the EG component between the center and edge of the droplet. Thus, the differences in the evaporation rates of the materials in the mixed solvent cause additional Marangoni flow from the outer rim to the center. The magnitude of the Marangoni flow is determined by the Marangoni number  $M = \Delta\gamma L / \eta_{AB} D_{AB}$ , where  $\Delta\gamma$  denotes the surface

tension difference between the center and edge of the droplet,  $\eta_{AB}$  is the viscosity of the mixed solvents,  $L$  is the length scale involved (i.e., the radius of the microdroplet placed on the substrate,  $\sim 2500 \mu\text{m}$ ), and  $D_{AB}$  is the diffusion coefficient in the binary solution.<sup>18</sup> The interdiffusion coefficient is obtained as  $D_{AB} = 7.4 \times 10^{-8} (\phi m_B)^{1/2} T / (\eta_B V_A^{0.6})$ , where A and B indicate the minor and major solvent species,  $m_B$  is the molecular weight of water,  $\eta_B$  is the viscosity of water,  $\phi$  is an association parameter, and  $V_A$  is the molar volume of the minor solvent.<sup>19</sup> The mixed viscosity  $\eta_{AB}$  was calculated by  $\ln \eta_{AB} = x_A \ln \eta_A + x_B \ln \eta_B + x_A x_B G_{AB}$ , where  $x$  is the mole fraction,  $G_{AB}$  is an interparameter, and  $\eta_A$  is the viscosity of EG. The calculated value of  $\eta_{AB}$  is  $10.3 \text{ mPa s}$ . Here, the pure values for the surface tension difference across the droplet are utilized. The calculated Marangoni number is about  $3.9 \times 10^6$  for the polyol Ag nanoparticle paste. This large Marangoni number indicates that sufficient inward flow occurs and thus the coffee-ring effect can be reduced. Based on these considerations, it is reasonable to observe the coffee-ring effect after deposition of aqueous-based Ag nanoparticles but to expect the observed depression of this effect after deposition of polyol-based Ag nanoparticle paste due to the increased Marangoni flow.

### Effect of Bonding Materials on Joint Microstructure

Figure 4 shows cross-sectional images of the joints using different Ag nanoparticles. There were obvious differences between the microstructures of the joints using different bonding nanomaterials. As shown in Fig. 4a, for the joints bonded using aqueous Ag nanoparticle paste, there was an obvious gap between the two Cu discs. The formation of the gap is related to the accumulation of Ag nanoparticles to the rim region due to the coffee-ring effect, as discussed above. Thus, the connection area was much smaller than the surface area of base metal. To reduce the disadvantages of segregation of the Ag nanopaste, dried nanoparticle powder can be used as the bonding material. Figure 4b shows a joint bonded using Ag nanoparticle powder. A dense Ag sintered layer formed between the two Cu discs after bonding when using Ag nanoparticle powder under pressure of 5 MPa. The coffee-ring effect totally disappeared, because these Ag nanoparticles were placed in solid form. It should be noted that agglomeration of the Ag nanoparticles will reduce the surface energy to some extent. As shown in Fig. 4b, obvious voids existed in the sintered Ag structure. This is expected since it is more difficult to get a dense structure when using solid bonding materials. Figure 4c illustrates a joint bonded using polyol Ag nanoparticle paste. It can be seen that a uniform and dense Ag layer was formed between the Cu discs. This indicates that the polyol Ag nanoparticle paste had better bondability than the aqueous Ag nanoparticle paste or powder.

### Effect of Bonding Materials on Joint Strength and Fracture Morphology

Figure 5 presents the shear strength of joints under the same bonding parameters using different bonding materials. The joints bonded by aqueous Ag nanoparticle paste and Ag nanoparticle powder had similar shear strength of 12 MPa. However, the average shear strength of the joints using polyol-based Ag nanoparticle paste was 50 MPa, which is significantly higher than those obtained using the aqueous-based materials. Thus, a drastic improvement of joint strength was achieved by controlling the uniform deposition of the bonding material.

The difference in joint strength is related to the coffee-ring effect and the interfacial microstructure that governs the interfacial strength between the sintered Ag layer and the plated Ag layer. Figure 6a displays SEM images of fracture microstructures of shear joints bonded using different bonding materials. As shown in Fig. 6a, dense microstructure was observed when using aqueous-based Ag nanoparticle paste as the bonding material. However, the connection area was much smaller than in the joints using Ag nanoparticle powder and polyol-based Ag nanoparticle paste. The small connection area is caused by the coffee-ring effect as discussed above. The coffee ring disappears when using the Ag nanoparticle powder as the bonding material. However, no obvious improvement of the shear strength was observed. This can be explained by the fracture microstructure of shear joints bonded using Ag nanoparticle powder. Although the Ag nanoparticles were sintered together, the sintered Ag layer had a low density and many voids still existed in the sintered Ag layer. Moreover, the joint was partially fractured at the interface between the sintered Ag layer and Ni/Ag-coated Cu discs, as shown in Fig. 6b. This indicates that the joint bonded using Ag nanoparticle powder was possibly just

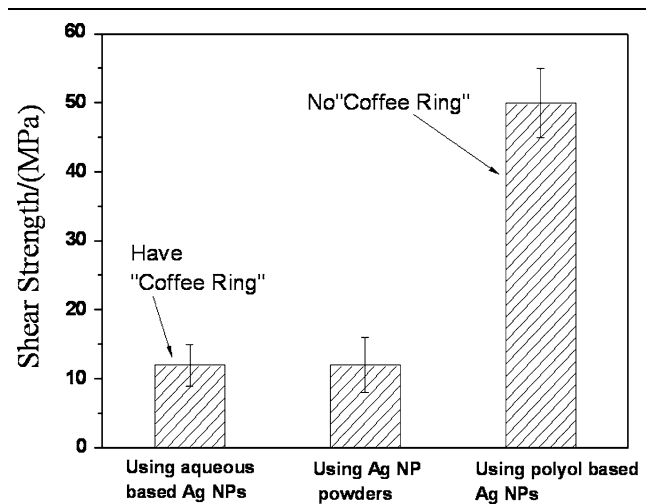


Fig. 5. Comparison of shear strength of joints bonded using different kinds of Ag nanoparticles.

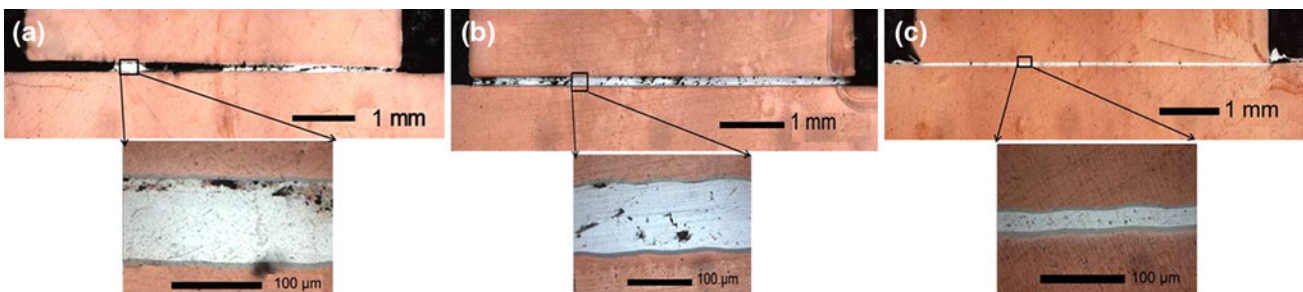


Fig. 4. Optical images of cross-sections of the joints using various bonding materials: (a) aqueous Ag nanoparticle paste, (b) Ag nanoparticle powder, and (c) polyol-based Ag nanoparticle paste.

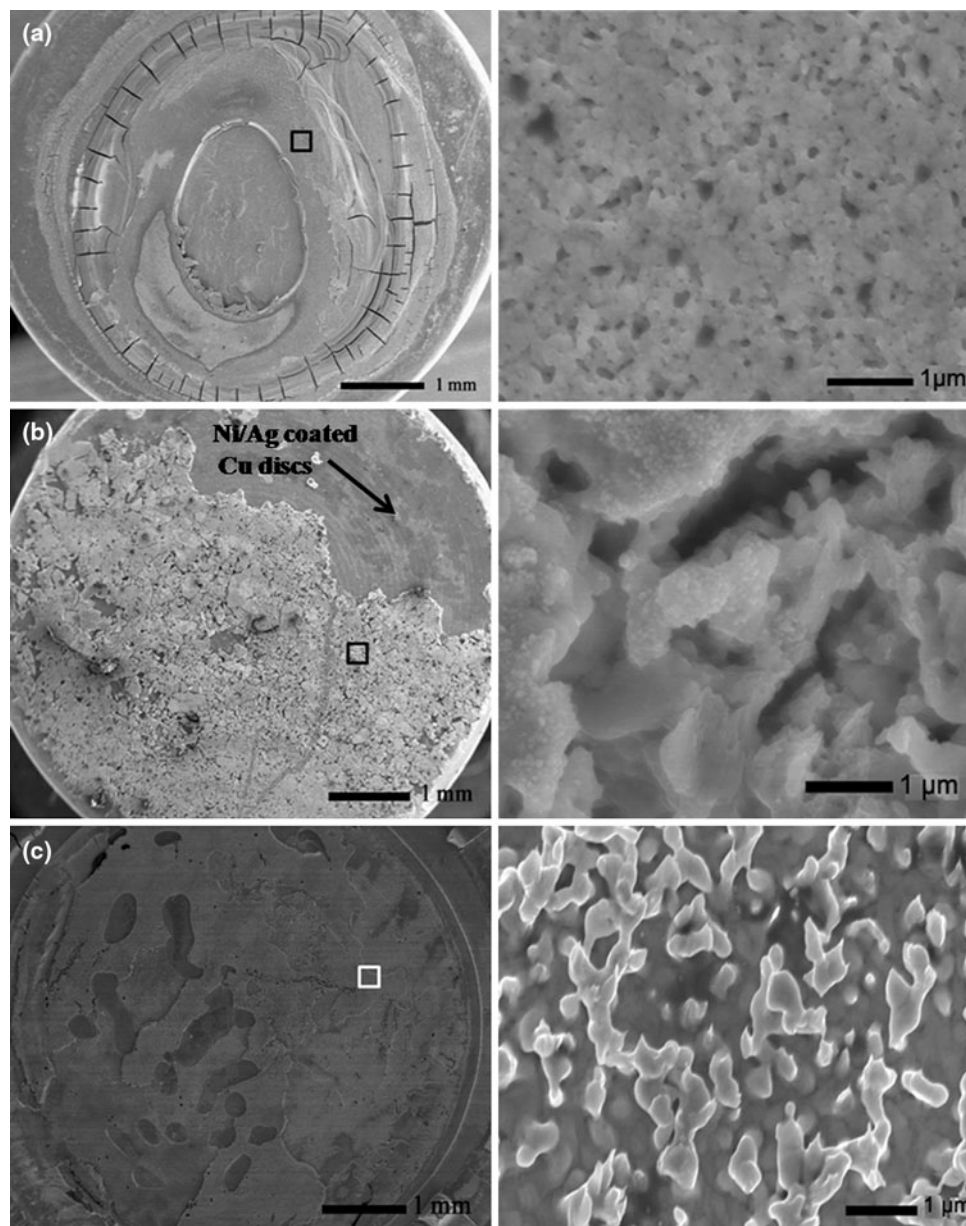


Fig. 6. SEM images of fracture microstructures of shear joints bonded using different bonding materials: (a) aqueous Ag nanoparticle paste, (b) Ag nanoparticle powder, and (c) polyol-based Ag nanoparticle paste.

physically rather than metallurgically bonded to the Ni/Ag-coated Cu discs.

A significant improvement of joint strength was achieved when the polyol Ag nanoparticles were used as the bonding material. Figure 6c presents corresponding SEM images of fracture microstructures of the shear joints. As discussed above, the coffee-ring effect was successfully depressed when using the polyol Ag nanoparticle paste. Thus, the corresponding connection area was increased. On the other hand, the sintered Ag layer had a denser microstructure. The joint was predominantly fractured in the sintered Ag layer. The fracture morphology confirms that the interfacial strength between the Ni/Ag-coated Cu disc and the sintered

Ag layer was improved. The tensile failure fracture traces indicate that some ductile behavior was achieved in the sintered Ag layer.<sup>20</sup> The above results show that the joint strength is improved by using polyol-based Ag nanoparticle paste as the bonding material.

## CONCLUSIONS

A sintering bonding method using both aqueous-based and polyol Ag nanoparticles has been investigated. In this sintering bonding process using Ag nanoparticles, the deposition behavior of the nanoparticle layer was critical to the joint formation. The coffee-ring effect had an obvious influence on the

behavior of the deposition and bondability of Ag nanoparticle paste. When aqueous-based Ag nanoparticle paste was used as the bonding material, the joint strength (12 MPa) was weak due to the coffee-ring effect. When using Ag nanoparticle powder as the bonding material the coffee ring disappeared, but there was not an obvious improvement in joint shear strength due to the presence of many voids in the sintered Ag structure. However, when using polyol-based Ag nanoparticle paste as the bonding material, the coffee-ring effect was depressed due to increased Marangoni flow. The corresponding joint shear strength was increased significantly to 50 MPa at low bonding temperature of 250°C. This sintering bonding technology using Ag nanoparticles as the interconnection material has potential applications in electronic packaging.

### ACKNOWLEDGEMENTS

This research was supported by the National Natural Science Foundation of China (Grant No. 51075232) and by Tsinghua University Initiative Scientific Research Program (Grant No. 2010THZ 02-1).

### REFERENCES

1. Y. Li, K. Moon, and C. Wong, *Science* 308, 1419 (2005).
2. M. Abteu and G. Selvaduray, *Mater. Sci. Eng. R* 27, 95 (2000).
3. K. Suganuma, *Curr. Opin. Solid. State Mater.* 5, 55 (2001).
4. H. Ogura, M. Maruyama, R. Matsubayashi, T. Ogawa, S. Nakamura, T. Komatsu, H. Nagasawa, A. Ichimura, and S. Isoda, *J. Electron. Mater.* 39, 1233 (2010).
5. E. Ide, S. Angata, A. Hirose, and K.F. Kobayashi, *Acta Mater.* 53, 2385 (2005).
6. Y. Zhou, eds., *Microjoining and Nanojoining* (Cambridge, UK: CRC/Woodhead, 2008).
7. J. Yan, G. Zou, A. Hu, and Y.N. Zhou, *J. Mater. Chem.* 21, 15981 (2011).
8. A. Hu, J.Y. Guo, H. Alarifi, G. Patane, Y. Zhou, G. Compagnini, and C.X. Xu, *Appl. Phys. Lett.* 97, 153117 (2010).
9. K.S. Moon, H. Dong, R. Maric, S. Pothukuchi, A. Hunt, Y. Li, and C. Wong, *J. Electron. Mater.* 34, 168 (2005).
10. Y. Lu, J.Y. Huang, C. Wang, S. Sun, and J. Lou, *Nat. Nanotechnol.* 5, 218 (2010).
11. H. Alarifi, A. Hu, M. Yavuz, and Y. Zhou, *J. Electron. Mater.* 40, 1394 (2011).
12. G. Zou, J. Yan, F. Mu, A. Wu, J. Ren, A. Hu, and Y.N. Zhou, *Open. Sur. Sci. J.* 3, 70 (2011).
13. Y. Sun and Y. Xia, *Science* 298, 2176 (2002).
14. R.D. Deegan, O. Bakajin, T.F. Dupont, G. Huber, S.R. Nagel, and T.A. Witten, *Nature* 389, 827 (1997).
15. R.D. Deegan, O. Bakajin, T.F. Dupont, G. Huber, S.R. Nagel, and T.A. Witten, *Phys. Rev. E* 62, 756 (2000).
16. H. Hu and R.G. Larson, *J. Phys. Chem. B* 110, 7090 (2006).
17. D. Pesach and A. Marmur, *Langmuir* 3, 519 (1987).
18. P. Takhistov and H.-C. Chang, *Ind. Eng. Chem. Res.* 41, 6256 (2002).
19. B.E. Poling, J.M. Prausnitz, and J.P. O'Connell, *Properties of Gases and Liquids*, 5th ed. (Blacklick: McGraw-Hill, 2001).
20. A. Hasnaoui, H. Van Swygenhoven, and P.M. Derlet, *Science* 300, 1550 (2003).